NASA CR-165200

SDL No. 80-2122-13F

FINAL REPORT

FOR

FUEL INJECTOR CHARACTERIZATION STUDIES

By

Michael J. Houser
William D. Bachalo

October 1980

Prepared for:

NASA LEWIS RESEARCH CENTER
21000 Brookpark Road
Cleveland, Ohio 44135

Under Contract No.
NAS3-21288

SPECTRON DEVELOPMENT LABORATORIES INC.

NASA CR-165200

SDL No. 80-2122-13F

FINAL REPORT

FOR

FUEL INJECTOR CHARACTERIZATION STUDIES

By

Michael J. Houser
William D. Bachalo

October 1980

Prepared for:

NASA LEWIS RESEARCH CENTER
21000 Brookpark Road
Cleveland, Ohio 44135

Under Contract No.
NAS3-21288

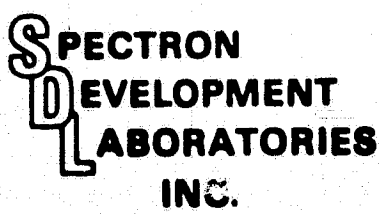

3303 Harbor Boulevard, Suite G-3
Costa Mesa, California 92626 (714) 549-8477

1. Report No.	2. Government Accession No.	3. Recipient's Catalog No.
NASA CR-165200		

4. Title and Subtitle	5. Report Date
FUEL INJECTOR CHARACTERIZATION STUDIES - FINAL REPORT	October 1980
	6. Performing Organization Code

7. Author(s)	8. Performing Organization Report No.
Michael J. Houser William D. Bachalo	SDL No. 80-2122-13F
	10. Work Unit No.

9. Performing Organization Name and Address	11. Contract or Grant No.
Spectron Development Laboratories, Inc. 3303 Harbor Boulevard - Suite G-3 Costa Mesa, California 92626	NAS3-21288
	13. Type of Report and Period Covered

12. Sponsoring Agency Name and Address	13. Type of Report and Period Covered
National Aeronautics & Space Administration Lewis Research Center Cleveland, Ohio 44135	Contractor Report
	14. Sponsoring Agency Code

15. Supplementary Notes

Project Manager, Michael Skorobatckyi, Engine Systems Division,
NASA Lewis Research Center, Cleveland, Ohio 44135

16. Abstract

This report describes an investigation to characterize the atomization of several general aviation piston engine manifold port fuel injectors. The injectors were installed in a test rig and operated under simulated conditions. Laser interferometric techniques were used to optically probe the spray droplet fields for droplet size and velocity at numerous spatial locations throughout the field.

17. Key Words (Suggested by Author(s))	18. Distribution Statement
Atomization Fuel Spray Measurement Droplet Sizing Fuel Injectors	Unclassified - Unlimited

19. Security Classif. (of this report)	20. Security Classif. (of this page)	21. No. of Pages	22. Price*
Unclassified	Unclassified		

* For sale by the National Technical Information Service, Springfield, Virginia 22161

TABLE OF CONTENTS

LIST OF FIGURES

LIST OF TABLES

1.0 INTRODUCTION

This report describes the work completed on the fuel spray characterization of a variety of commercial fuel injectors, as part of a NASA Lewis Research Center Program of research and technology development related to general aviation aircraft engines. Overall, the program has the objective of establishing and demonstrating the technology that can safely reduce the fuel consumption and emissions of aviation piston engines.

Improvements in the combustion efficiency can be achieved through improvements to the fuel/air preparation prior to combustion. There is a substantial influence resulting from the mean and turbulent flow characteristics in the mixing chamber and in the combustion on the energy release and pollutant formation. Thus, a thorough documentation of the fuel/air mixing including the droplet size distribution, fuel droplet and air velocities, size-velocity correlations, number densities and spatial distributions are vital to the development of energy efficient engines.

In the present report, eight commercial spark-ignition engine manifold port fuel injectors were tested at five test conditions each. Three of the simulated manifold test conditions were idle, takeoff, and cruise for all eight injectors. The remaining two test conditions varied depending on the type of injector being tested. Data were obtained at sixty spatial locations for each injector test condition. The Spectron Droplet Sizing Interferometer (DSI) was utilized in the acquisition of these data which included the size and velocity distributions and the

size-velocity correlations. These data are unique in that previous nonintrusive techniques could not provide simultaneous size and velocity measurements in high number density sprays.

A brief description of the measurement technique is given in the next section along with that of the test facility. The test procedures and data acquisition matrices are also documented in this section. Comments and discussion of the data are given to assist the user in evaluating the data and to provide explanations of any discrepancies. Some recommendations for future work are also given.

2.0 APPARATUS DESCRIPTION

In the following sections, the instrumentation, test rig, and fuel injectors are described.

2.1 Droplet Sizing Interferometer

The droplet sizing interferometer (DSI) was devised by Bachalo (Appendix II) to fulfill the need to make simultaneous droplet size and velocity measurements in high number density sprays. This method is essentially a laser Doppler velocimeter with the additional capability of being able to measure the droplet size. Figure 1 is the optical configuration required in the utilization of the technique. Briefly, the laser beam is partitioned into two equal intensity beams and then focused to a crossover region. Light scattered by droplets passing through the crossover region is collected by the receiving system situated at some off-axis angle (e.g., 30°). The intersection of the image of the photomultiplier tube aperture and the focused beams forms a very small probe cross-section allowing measurements in high number density sprays. A detailed description of the method is given in the paper included in Appendix II.

With this method, the droplet velocity is determined from the Doppler period (high frequency component) of the signal (Figure 2) using the following expression

$$U(d_i,t) = \delta\, f_D \qquad (1)$$

where δ is the interference fringe spacing in the probe volume and f_D is the Doppler frequency. Droplet size is obtained from the same signal

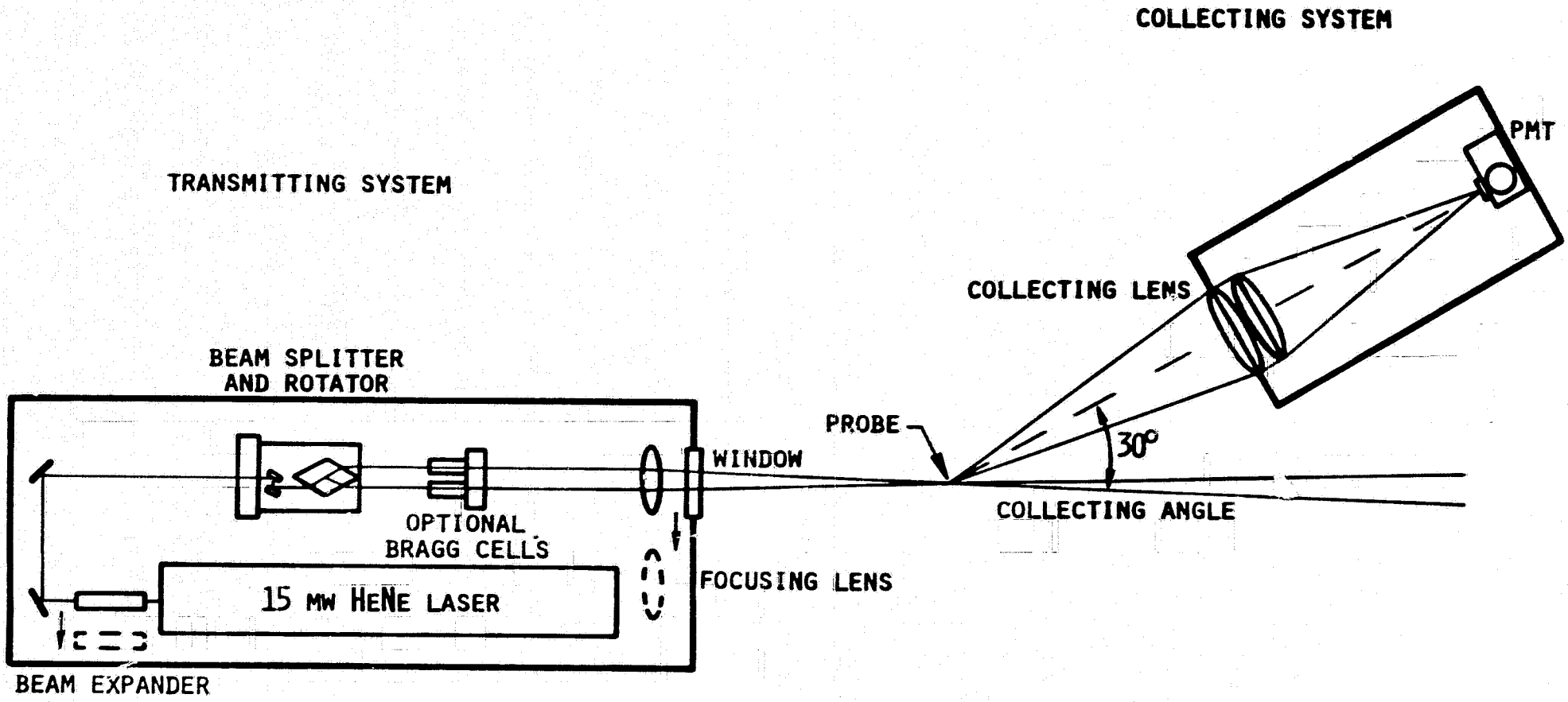

FIGURE 1. OPTICAL CONFIGURATION OF THE INSTRUMENT.

80-6577-5-0

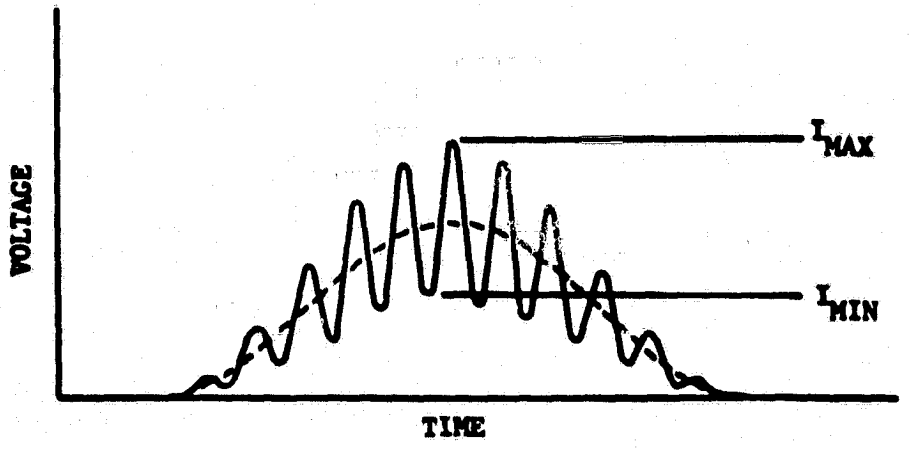

(A) DOPPLER BURST SIGNAL

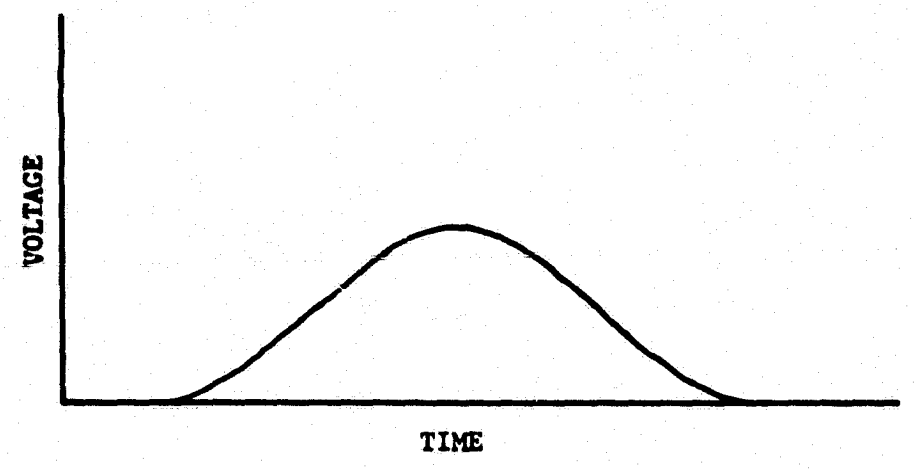

(B) PEDESTAL COMPONENT

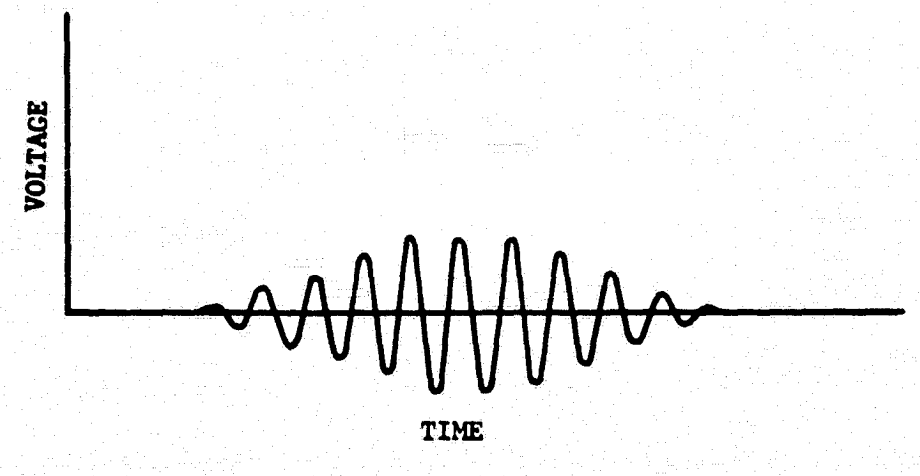

(C) DOPPLER COMPONENT

FIGURE 2. DOPPLER BURST SIGNAL SHOWING THE DOPPLER AND PEDESTAL COMPONENTS.

by measuring the signal visibility which is the ratio of the Doppler component (Figure 2) to the pedestal component. The visibility is then related to the dimensionless parameter, d/δ. In addition to producing the measurement of the size and velocity for each droplet passing through the probe volume, the size determination is not affected by attenuation of the laser beam or the scattered light. This is an important feature when measuring in dense sprays and combustion environments.

2.2 Measurement Capabilities

Velocity

The measurement of the gas phase and droplet velocities in cold sprays with the DSI instrument produced by Spectron Development Laboratories is relatively straightforward. Gas phase velocity is obtained by measuring the period of the Doppler burst signal obtained from small particles (1-2 μm) that will adequately respond to the turbulent fluctuations of the gas phase. When obtaining these measurements in the presence of fuel sprays, the simultaneous measurement of the particle size is required. Otherwise, it is impossible to separate signals from droplets which may not respond to the gas phase motions. The on-line signal processing and data management computer is capable of storing the size and velocity of each droplet passing through the measurement volume at rates as high as 10,000/sec. These data pairs are stored directly in memory and later analyzed to produce the droplet and gas phase velocities and the size-velocity correlations.

By orientating the interference fringe pattern in two orthogonal directions, the streamwise (U) and transverse (V), velocity components can be determined. With the additional size information, the accumulated velocities can be separated by size increment. Thus, $U(d_i,t)$, $V(d_i,t)$ are obtained where the d_i are the droplet size increments and t indicates that these are instantaneous realizations. Assuming that the air flow and spray velocities are statistically stationary, the time averages are used to obtain the mean and rms fluctuating velocity for each size increment. That is

$$\overline{U}\,(d_i) = \sum_{j=1}^{N} \frac{U_j\,(d_i,t)}{N} \qquad (2)$$

and $$\langle U'\,(d_i)\rangle \sqrt{\overline{U'^{2}}\,(d_i,t)} = \left|\sum_{j=1}^{N} \left(\frac{U_j^{2}}{N}\,(d_i,t) - \overline{U}\,(d_i)\right)\right|^{1/2} \qquad (3)$$

Typically, 3,000 instantaneous droplet measurements are used to produce the probability density distributions used.

The measurement of the transverse velocity components and in recirculation regions usually requires frequency shifting. Frequency shifting causes the interference fringe patterns to appear to move at the shift frequency. This frequency offset allows the measurement of the small traverse velocity component and the resolution of the directional ambiguity in recirculating flows. With frequency shifting the velocity is

$$U(d_i,t) = \frac{\left(f_D(d_i,t) - f_s\right)}{2 \sin \theta/2} \lambda \qquad (4)$$

where f_D is the Doppler frequency and f_s the shift frequency.

Droplet Size

The individual droplet size measurements are accumulated in histogram form to obtain the size distribution and the various mean diameters. Various mean diameters used in spray analysis including the linear, surface, volume, and Sauter mean diameters are obtained from the following expression:

$$\bar{d}_{qp} = \left[\frac{\sum_{i=1}^{N} d_i^q}{\sum_{i=1}^{N} d_i^p}\right]^{\frac{1}{q-p}} \qquad (5)$$

For example, $\bar{d}_{10}$ is the linear mean and $\bar{d}_{32}$ is the Sauter mean diameter.

Fuel flow or droplet number density can also be evaluated since the measurement cross-section is defined and the number and size of particles passing the measurement cross-section per unit time is measured.

Simultaneous measurement of the droplet size and velocity of the droplets allows evaluation of the droplet size-velocity correlations. These data describe the response of the various droplet sizes to the prevalent gas phase conditions. Response of the relative droplet sizes can be used, for example, to estimate the probability of downstream droplet collisions and the relative droplet Reynolds number. High relative Reynolds number will induce circulation within the droplet which in turn increases the heat exchange and reduces the chance of droplet evaporation. The velocity of the gas phase relative to the fuel will increase the local oxygen supply to the fuel and the removal of the vaporized fuel from around the fuel droplet.

2.3 Description of the Test Facility

The test rig and facilities for this program were provided by the General Electric Aircraft Engine Group. Because of the high volumetric flowrates required in this test, the General Electric facilities were deemed most suitable.

A schematic drawing of the fuel injector test rig is presented in Figure 3. Photographs of the test rig installed in the combustion laboratory test cell are presented in Figures 4 and 5. The test section assembly consisted of an inlet transition duct, a square test section and an exit transition duct that was identical to the inlet duct. A design drawing of the transition section is presented in Figure 6. This duct was 18 inches long with an 8-inch diameter pipe flange at the inlet end and a 10-inch square section flange at the exit end of the duct. The test section drawing is presented in Figure 7. This section was 10 inches square and 24 inches long with two 8-inch by 11-inch rectangular windows

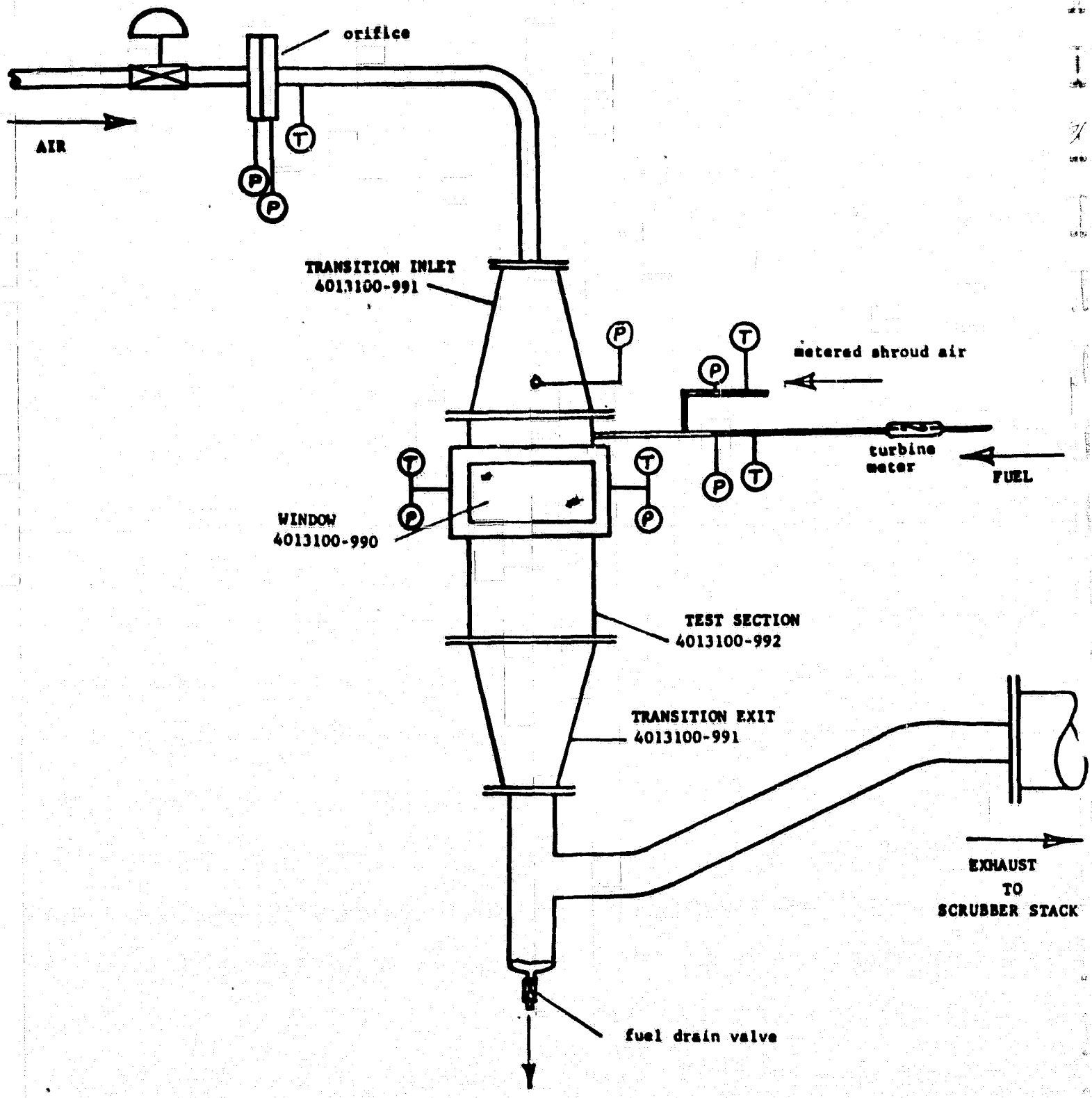

FIGURE 3. FUEL INJECTOR TEST RIG SCHEMATIC

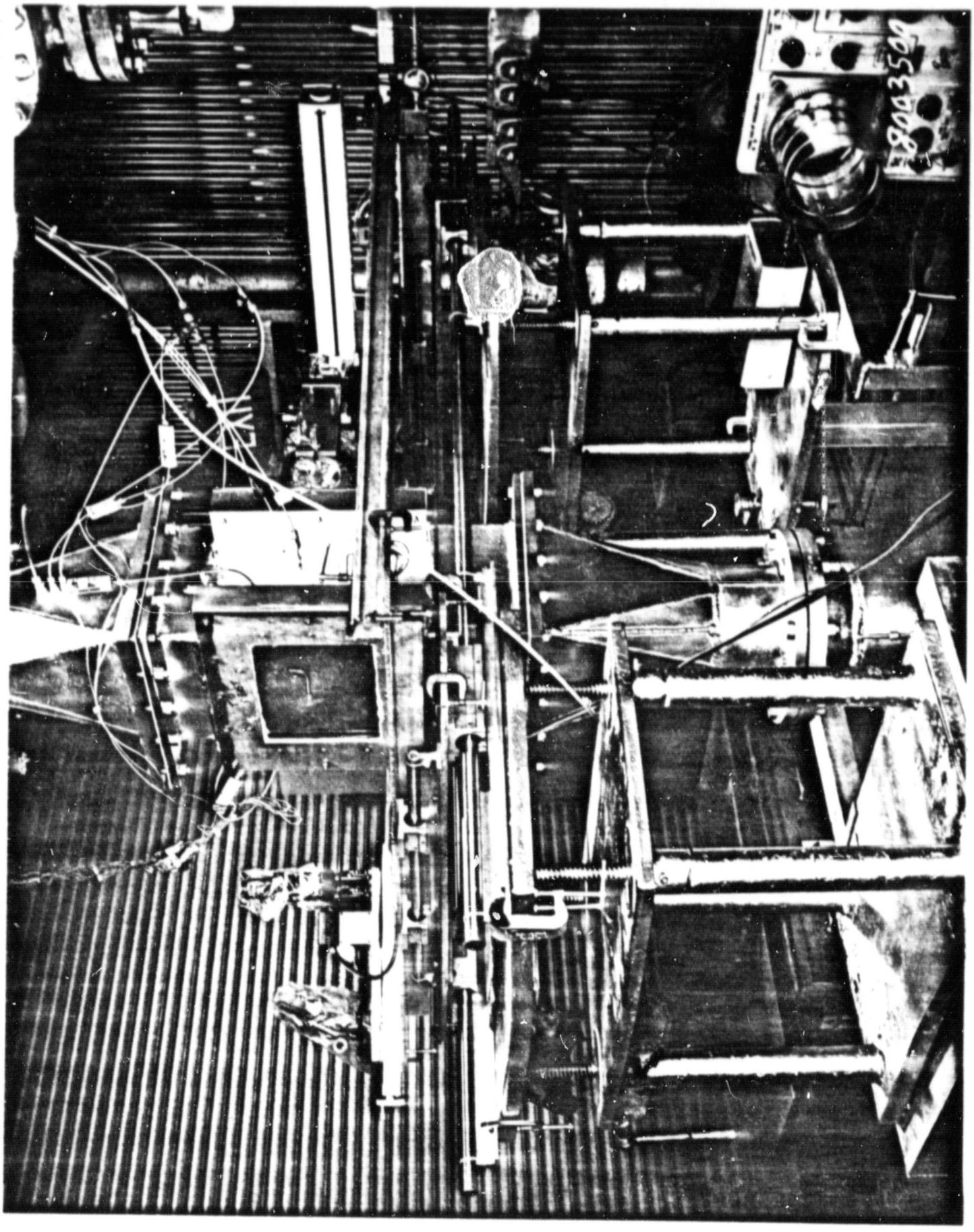

FIGURE 4. FUEL INJECTOR TEST RIG INSTALLED IN TEST CELL

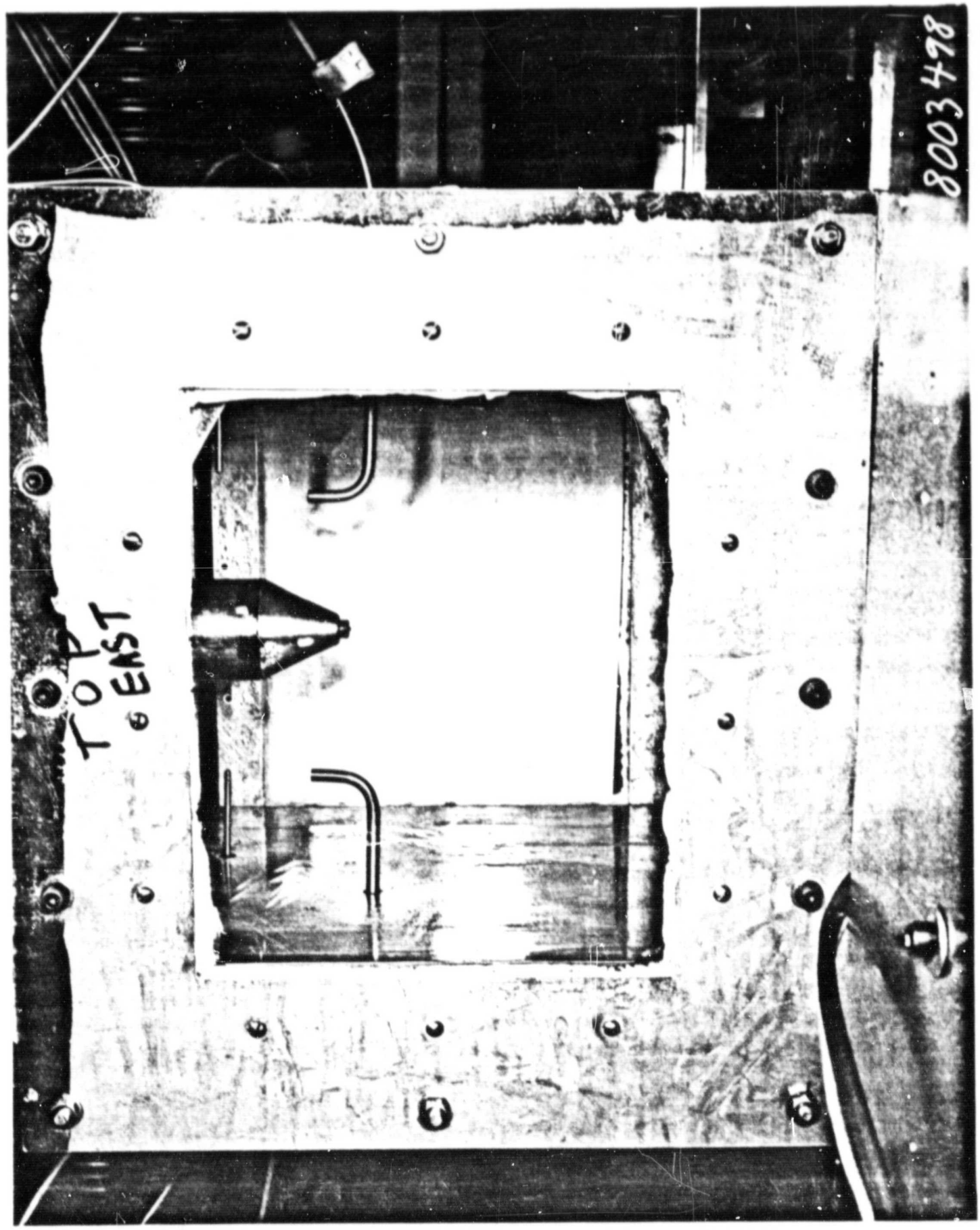

FIGURE 5. TEST SECTION OF FUEL INJECTOR TEST RIG

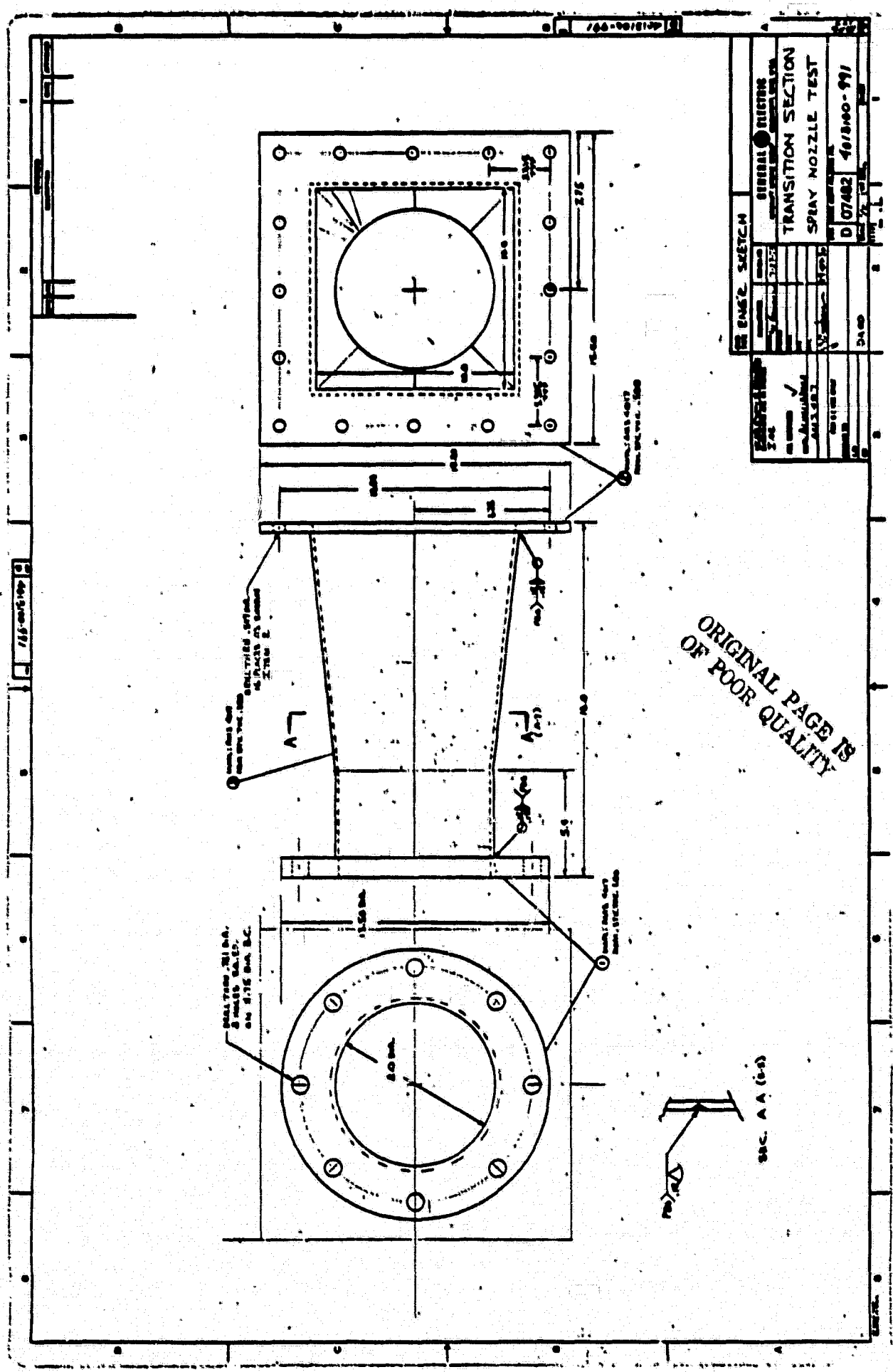

FIGURE 6. TRANSITION SECTION

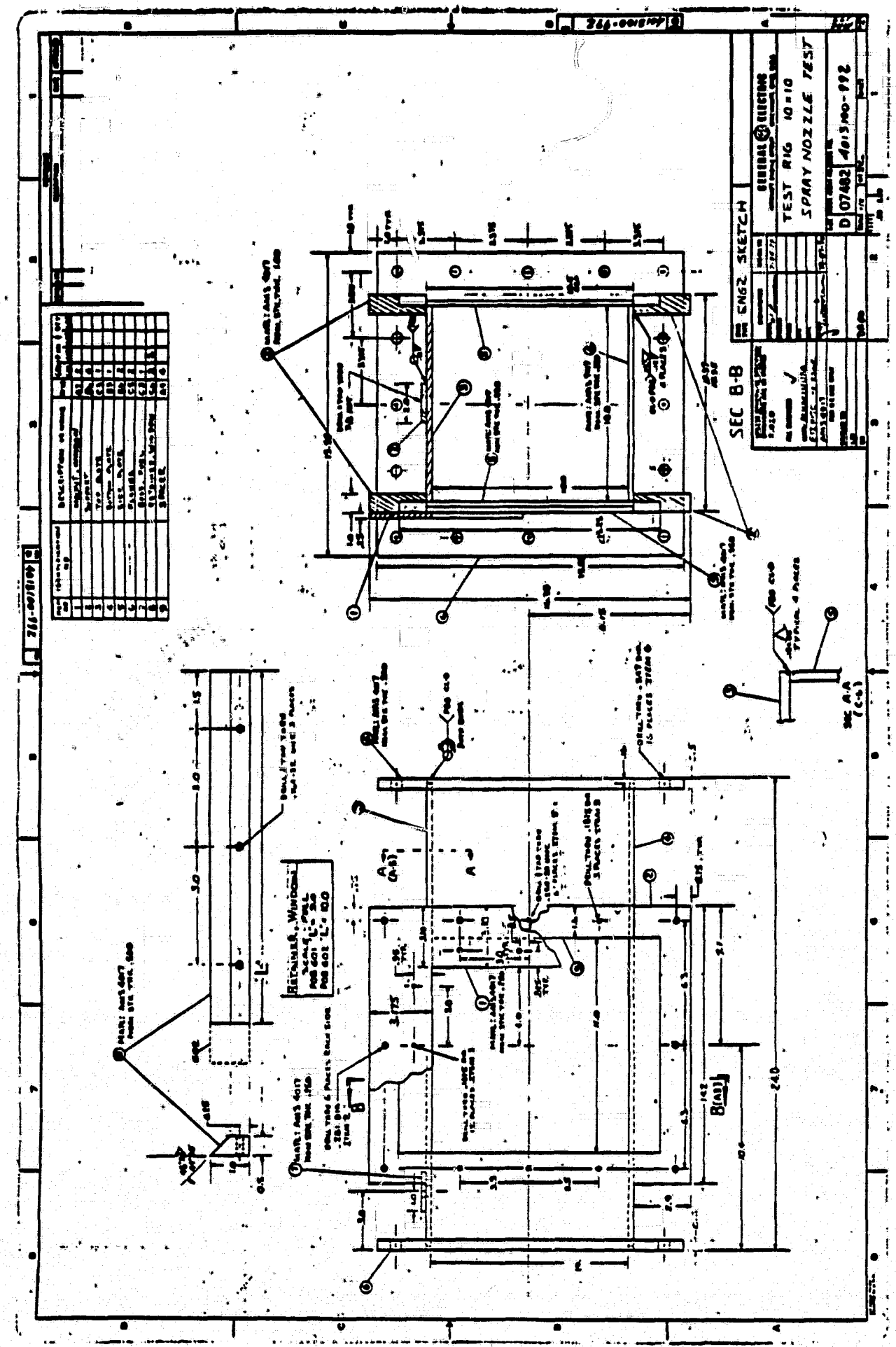

FIGURE 7. TEST SECTION

on opposite sidewalls. Optical quality glass is used for the windows with a surface flatness of one-half wave length per inch.

A standard ASME orifice plate was used to measure the airflow entering the test rig. The airflow then passed through a large filter to remove all traces of oil from the air ahead of the test rig. The fuel injectors were mounted in a streamlined fuel injector holder that was designed to minimize wake regions downstream of the fuel injection point. This holder design is illustrated in Figure 8.

Fuel pressure and fuel temperature were measured at the entrance to the test rig. Airflow, total pressure, static pressure, and total temperature were measured at the fuel injection plane.

After leaving the test section, the fuel and air mixture turned through a 90-degree pipe section and passed through a straight pipe to a steam ejector which was used to obtain low pressure levels in the test section. The fuel-air mixture then passed through a fuel scrubber stack to remove the fuel before the flow was exhausted to the atmosphere. Liquid fuel from the test section was continuously drained through a fuel drain valve ahead of the 90-degree pipe section.

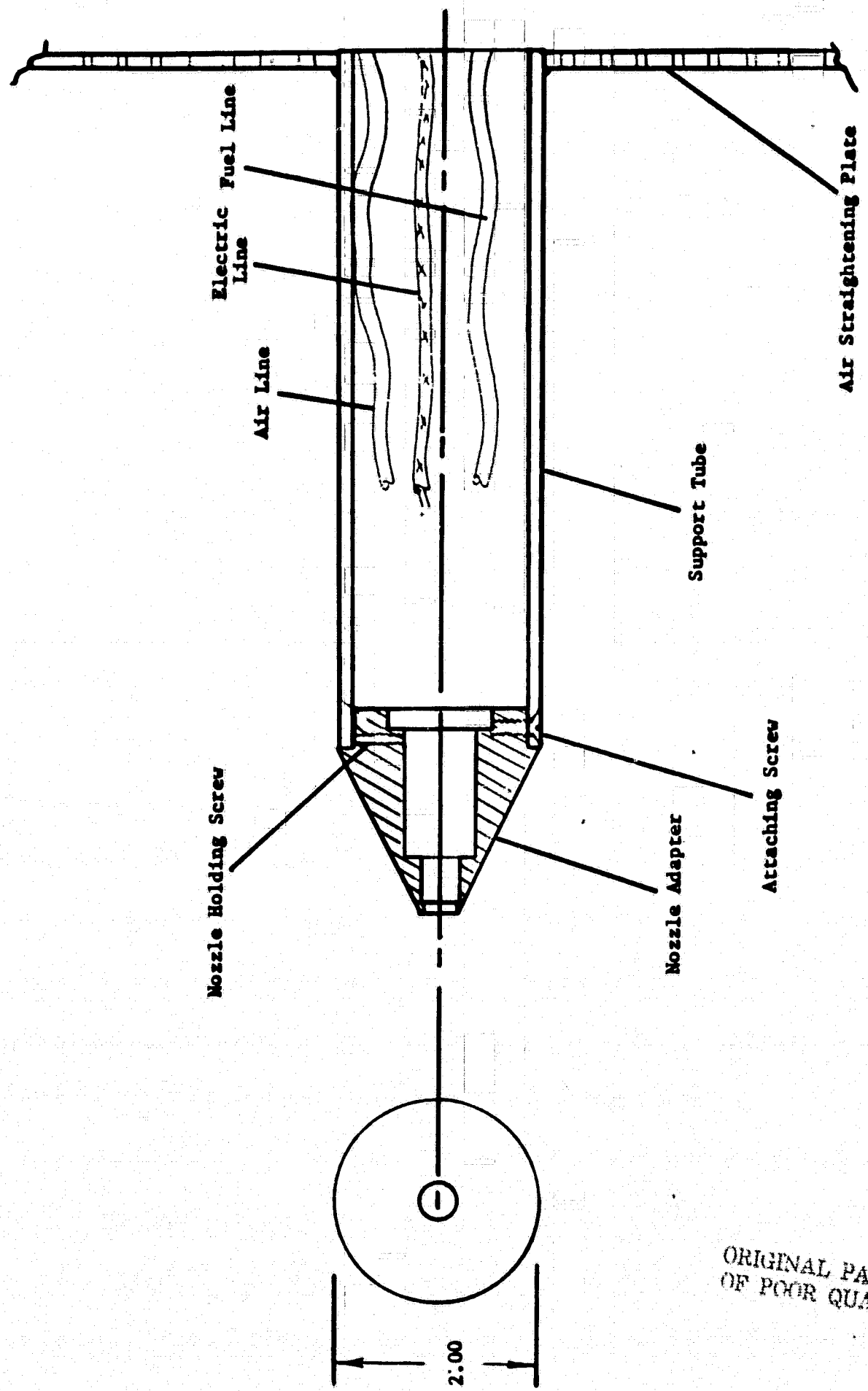

FIGURE 8. FUEL-INJECTOR SUPPORT STRUCTURE

3.0 PROCEDURE

3.1 Fuel Analysis

The fuel was purchased in a lot of 500 gallons. Commercial grade 100/130 octane aviation fuel was acquired for the test as specified in the RFP. Tests were conducted by General Electric personnel to obtain the specific gravity, viscosity and the surface tension of the fuel at 75°F. In addition, the index of refraction which was required for the droplet size measurements was also measured. The fuel analysis results are given below as Table 1.

TABLE 1

GRADE 100/130 AVIATION GASOLINE	
Values at 23.9°C (75°F)	
Specific Gravity	0.6895
Viscosity	6.2×10^{-7} m^2/s
Surface Tension	2.1×10^{-2} nt/m
Refractive Index	1.3906

3.2 Nozzle Calibration

The eight (8) fuel injectors were individually tested to determine fuel pressure when a fuel flowrate was specified or flowrate when a fuel pressure was specified. These tests were done in the G.E. Nozzle Test Laboratory with the results tabulated in Table 2.

TABLE 2

TEST POINT	INJECTOR	FUEL FLOW lb/hr (kg/hr)	FUEL PRESSURE psig (nt/m^2)
1	BENDIX-74151	1.2 (2.6)	* (*)
2		11.6 (25.6)	4.5 (3.1×10^4)
3		20.0 (44.1)	7.0 (4.8×10^4)
4		1.2 (2.6)	* (*)
5		11.6 (25.6)	4.5 (3.1×10^4)
6	TCM-63308-13E	1.3 (2.9)	* (*)
7		13.0 (28.7)	2.5 (1.7×10^4)
8		24.0 (52.9)	8.2 (5.7×10^4)
9		1.3 (2.9)	* (*)
10		13.0 (28.7)	2.5 (1.7×10^4)
11-15	BENDIX-1606771	39.7 (87.5)	40.0 (2.8×10^5)
16-20	BENDIX-1607247	49.9 (110.0)	40.0 (2.8×10^5)
21-25	LUCAS-073143	41.8 (92.2)	40.0 (2.8×10^5)
26-30	SIMMONDS-571341	221.0 (487.3)	80.0 (5.5×10^5)
31-35	BOSCH-0437-502-004	10.0 (22.1)	48.0 (3.3×10^5)
36-40	BOSCH-0280-150-191	25.1 (55.3)	40.0 (2.8×10^5)

* These values below sensitive range of the instrumentation

During the course of the tests, the injector condition given in the test matrix (pressure or flowrate) was set. A turbine vane flowmeter was used to measure flowrates during the testing. The low flowrates were achieved by utilizing a rotometer in the fuel line.

3.3 Airflow Uniformity Test

Tests were conducted early in the program to insure that the airflows generated in the test rig were uniform across the test section. A pitot probe was used for this test. The results of that test are given in the included matrix (Table 3).

Additional tests were made which showed that some of the desired air velocities (225 f/s, 260 f/s) could not be achieved in the test rig due to the prohibitive air mass flows required. Since shear between the airflow and the injector droplets is dependent upon their relative velocity, a method of increasing the air velocity was devised. The rig was fitted with a close mesh screen at the inlet to the 10" x 10" test section. The screen had a 6" diameter hole in its center to allow free flow of air in the vicinity of the nozzle while restricting the airflow at the periphery of the test section. This resulted in non-uniform flow at the plane of the nozzle, but increased air velocity near the nozzle exit.

3.4 Nozzle Test Matrix

Tests were made on eight (8) fuel nozzles with five (5) different operating conditions on each. The fuel/air preparation test matrix is shown in Appendix I, representing the forty (40) injector test points. At each test point, data was taken at six (6) horizontal planes representing varying downstream distances from the injector exit. In each plane, ten (10) individual spatial points were selected to represent the spray condition in that plane. At each spatial point, 3,000 data samples were taken for both droplet size and velocity.

TABLE 3

NASA-LEWIS INJECTOR TEST RIG

AIR INLET →

PI	Δp	T	Wa
Psi	"H_2O	F°	PPS
80	60	45	2.0

Orifice (Shop) = 2.416"

PROBE POS.	TUNNEL PRESSURE LOCATION ("H_2O) 1"	2"	3"	4"	5"	6"	7"	8"	9"
.5	7.0	6.8	6.8	6.8	6.7	6.8	6.8	6.8	6.9
1.0	6.9	6.8	6.8	6.8	6.8	6.8	6.9	6.9	6.9
1.5	7.0	6.9	6.8	6.8	6.8	6.8	6.9	6.9	6.9
2.0	7.0	6.8	6.8	6.9	6.9	6.9	6.9	7.0	6.9
2.5	6.8	6.8	6.9	6.9	7.0	6.9	7.0	7.0	6.9
3.0	6.9	6.8	6.9	7.0	7.0	7.0	7.1	7.1	7.1
3.5	6.8	6.9	6.9	7.0	7.0	6.9	7.1	7.2	7.3
4.0	6.9	7.0	6.9	7.0	7.0	7.0	7.2	7.3	7.3
4.5	7.1	7.0	7.0	7.0	7.1	7.1	7.2	7.4	7.4
5.0	7.0	6.9	7.0	7.0	7.1	7.1	7.2	7.4	7.5
5.5	6.8	7.0	7.0	7.0	7.1	7.1	7.3	7.4	7.5
6.0	7.0	7.0	7.1	7.1	7.0	7.2	7.3	7.5	7.6
6.5	6.9	6.9	6.9	7.1	7.1	7.2	7.3	7.4	7.6
7.0	7.0	6.9	6.9	7.1	7.0	7.1	7.3	7.5	7.6
7.5	6.9	6.9	6.9	7.1	7.1	7.1	7.3	7.5	7.6
8.0	6.9	6.9	6.9	7.0	7.1	7.1	7.3	7.5	7.7
8.5	7.0	6.9	7.0	7.0	7.0	7.2	7.4	7.5	7.7
9.0	6.9	6.9	7.0	7.0	7.1	7.2	7.3	7.3	7.6
9.5	6.8	6.8	6.9	7.0	7.1	7.1	7.3	7.2	7.4
10.0	6.8	6.9	6.8	6.9	7.0	7.0	7.2	6.9	7.1
$\frac{Ps}{("H_2O)}$	6.5	6.5	6.5	6.5	6.5	6.5	6.5	6.5	6.5

The injector test points were chosen to simulate various piston engine operating conditions. Changes in fuel flow, fuel pressure, tunnel air pressure, tunnel air speed, and shroud air pressure were made to compare injector atomization over portions of the EPA five-mode aircraft operating cycle. The injectors were standard, commercially available models; 4 mechanically operated and 4 electrically operated. The electronic nozzles were run with the required operating voltage constantly applied during the test (injector always open).

The test planes below the injector exit were nominally 0.5", 1.0", 1.5", 2.0", 3.0", 4.0". Within each plane, 10 spatial locations were selected by the operator to most fully describe the flow in the plane. Spray boundaries in at least two directions were made with the remaining points distributed along one or two radii of the spray. At times, complete non-symmetry of the spray made the best selection of spatial points difficult.

4.0 RESULTS

4.1 Test Point Conditions

The fuel/air preparation test matrix is found in Appendix I along with the actual settings of the nozzle test rig and readings of the rig flow instrumentation. Abbreviation of the test points occurs throughout the results. These abbreviations are explained in Table 4. The test rig airflow was set by way of pressure drop across an orifice plate. Air mass flow was read from the orifice calibration curve. Test section diagnostics (total pressure, static pressure, temperature) were made at the nozzle exit plane simultaneously on opposing (North, South) walls. Fuel flow was set by pressure or flowrate as mandated by the test matrix. A turbine vane flowmeter was placed in the fuel line to measure fuel flow. Its calibration curve gave lbm/hr fuel as a function of vane rotations/second.

TABLE 4

TEST POINT NOMENCLATURE

TEST POINT	ABBREVIATED NOMENCLATURE	INJECTOR
1	B1	BENDIX - 74151 Air-Assisted, Mechanical
2	B2	
3	B3	
4	B4	
5	B5	
6	T6	TCM - 63308-13E Air-Assisted, Mechanical
7	T7	
8	T8	
9	T9	
10	T10	
11	B11	BENDIX - 1606771 Electronic
12	B12	
13	B13	
14	B14	
15	B15	
16	B16	BENDIX - 1607247 Electronic
17	B17	
18	B18	
19	B19	
20	B20	
21	L21	LUCAS - 073143 Electronic
22	L22	
23	L23	
24	L24	
25	L25	
26	S26	SIMMONDS - 571341 Mechanical Pintle
27	S27	
28	S28	
29	S29	
30	S30	
31	B031	BOSCH - 0437-502-004 Mechanical Pintle
32	B032	
33	B033	
34	B034	
35	B035	
36	B036	BOSCH - 0280-150-151 Electronic
37	B037	
38	B038	
39	B039	
40	B040	

4.2 Individual Spatial Data

This data is found on a point-by-point basis in the Comprehensive Data Report (SDL No. 80-2122-13C). The droplet size data is both plotted and listed on each printout. Also found on the computer listings are the various mean diameter calculations and the size-velocity correlation results. The listings are explained in Figure 10 and the formulae for the mean calculations are given in Figure 11.

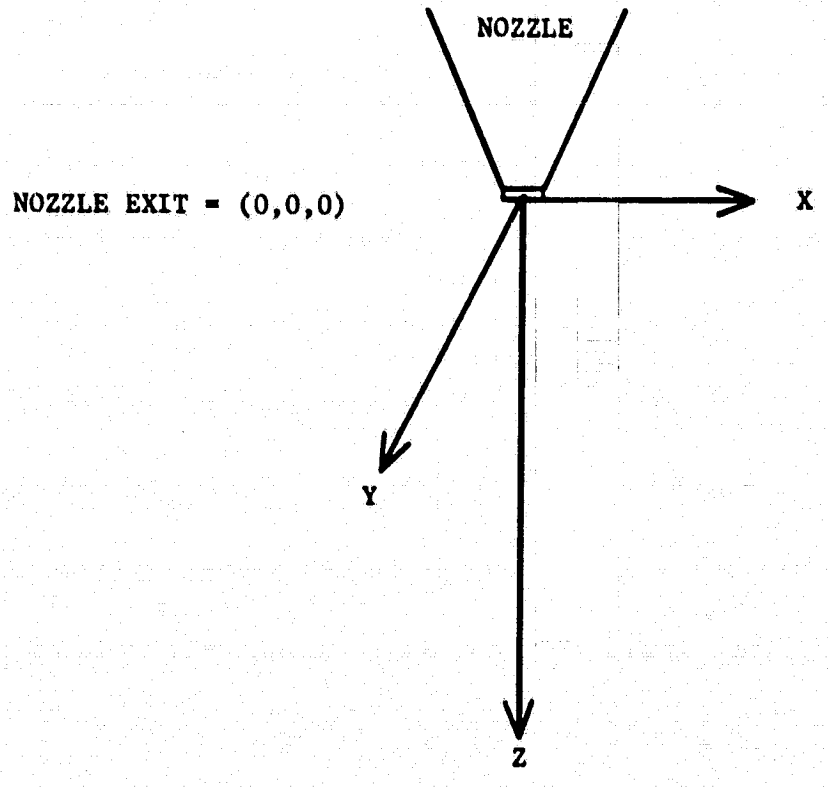

FIGURE 9. COORDINATE SYSTEM

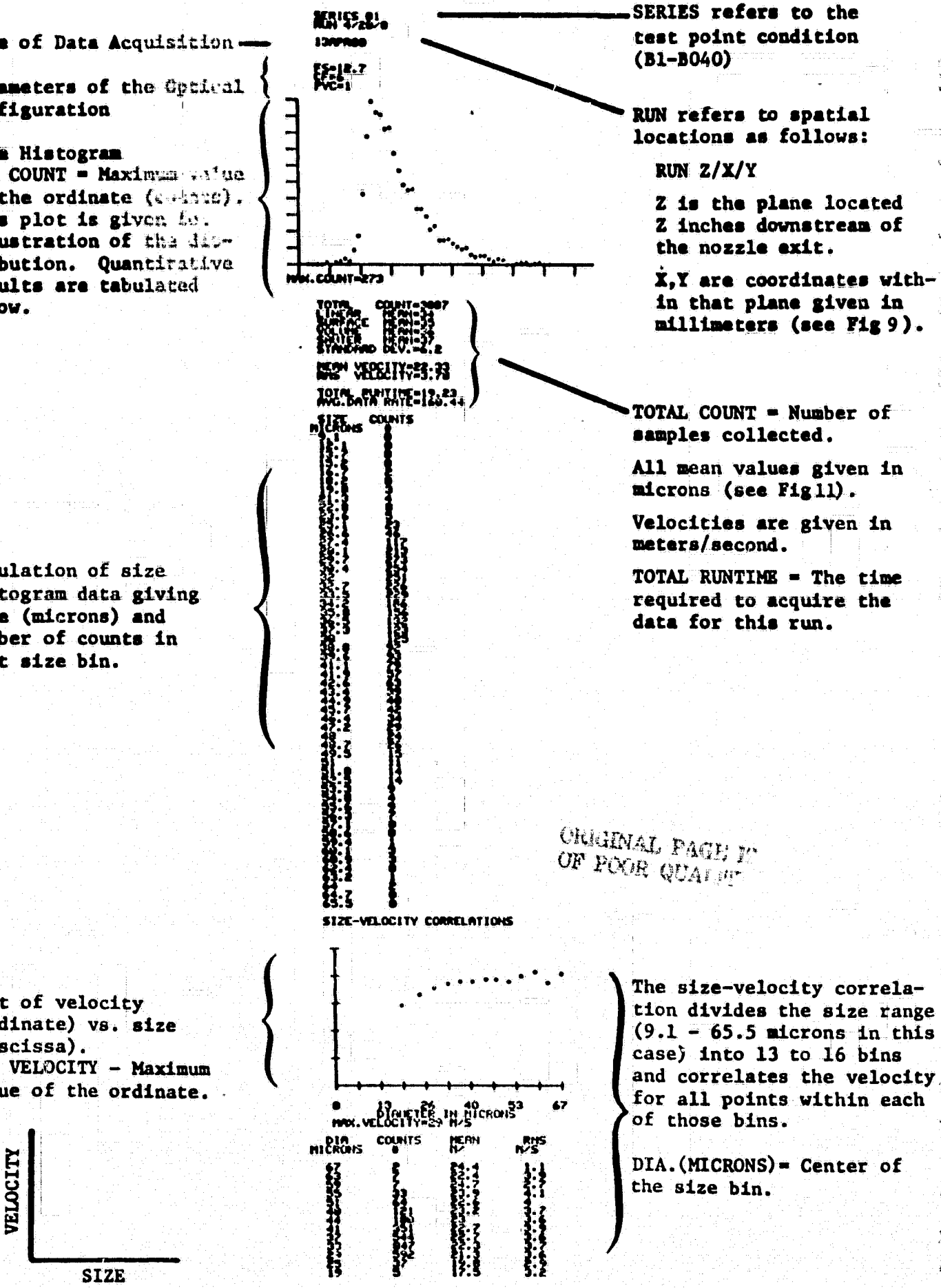

FIGURE 10. COMPUTER LISTING FORMAT

N_T = TOTAL NUMBER OF BINS

n_i = NUMBER OF COUNTS IN BIN i

d_i = DIAMETER OF DROPLETS IN BIN i

u_i = VELOCITY OF DROPLETS IN BIN i

$T_c = \sum_{i=1}^{N_T} n_i$ = TOTAL NUMBER OF COUNTS IN ALL BINS

LINEAR MEAN DIAMETER, $d_o = \frac{1}{T_c} \sum_{i=1}^{N_T} d_i \, n_i$

SURFACE MEAN DIAMETER = $\frac{1}{T_c} \left(\sum_{i=1}^{N_T} d_i^{\,2} \, n_i \right)^{1/2}$

VOLUME MEAN DIAMETER = $\frac{1}{T_c} \left(\sum_{i=1}^{N_T} d_i^{\,3} \, n_i \right)^{1/3}$

SAUTER MEAN DIAMETER = $\dfrac{\sum_{i=1}^{N_T} d_i^{\,3} \, n_i}{\sum_{i=1}^{N_T} d_i^{\,2} \, n_i}$

STANDARD DEVIATION = $\left(\frac{1}{T_c} \sum_{i=1}^{N_T} n_i \, (d_i - d_o)^2 \right)^{1/2}$

MEAN VELOCITY, $\bar{u} = \frac{1}{T_c} \sum_{i=1}^{N_T} u_i \, n_i$

RMS VELOCITY = $\left(\frac{1}{T_c} \sum_{i=1}^{N_T} n_i \, (u_i - \bar{u})^2 \right)^{1/2}$

FIGURE 11. STATISTICAL FORMULAE

4.3 Planar Data

A summary of spatial data is presented in the planar plots of the Comprehensive Data Report (SDL No. 80-2122-13C). These plots show the locations of the individual data points and restate the linear mean diameter and mean velocity at each point. Points on the perimeter of the spray field are denoted (SB) for spray boundary. Questionable data are indicated by an asterisk (*). These data are in doubt due to errors in acquisition or raduction, excessively high droplet number densities, or the determination by the operator that the spray had not yet broken up into droplets. Also included on the planar data sheets is a simple mean calculation meant to represent an average value for the entire plane.

4.4 Nozzle Averages

A further compression of droplet size and velocity data is given in the nozzle averages of Table 5. This table allows a rapid comparison of planar averages for each nozzle along with nominal air velocity and nozzle pressure drop for each condition. Air velocities are converted to meters/sec to compare with measured droplet velocities. Also, the addition of an upstream screen to the test section inlet (see Section 3.3) should have had a large effect on air velocities although this effect was not characterized.

Of the 40 nozzle conditions investigated, only test point 4 failed to produce an atomized spray. As such, no data was obtained from this condition and no results appear in this section.

TABLE 5a. - Nozzle Averages

TEST CONDITION	PLANE INCHES	MEAN DIA. μM	MEAN VEL. (M/S)
B1	4	34	22.0
	3	40	24.0
Δp=9.0 psia	2	43	27.0
V=16.7 m/s	1.5	45	31.0
	1	45	32.0
	.5	DENSE SPRAY	
B2	4	55	60.8
	3	55	57.1
Δp=7.2 psia	2	55	45.8
V=68.6 m/s	1.5	55	40.0
	1	52	33.0
	.5	50	18.0
B3	4	60	56.2
	3	58	53.0
Δp=7.9 psia	2	58	46.3
V=79.2 m/s	1.5	56	41.4
	1	55	34.0
	.5	53	17.4
B5	4	41	58.7
	3	41	56.0
Δp=negligible	2	41	47.2
V=68.6 m/s	1.5	40	42.3
	1	36	27.3
	.5	-	26.0
T6	4	43	15.1
Δp=5.6 psia	2	40	13.3
V=16.7 m/s			
T7	4	57	58.6
Δp=1.8 psia	2	55	46.0
V=68.6 m/s			
T8	4	44	51.5
Δp=5.0 psia	2	44	39.4
V=79.2 m/s			
T9	4	29	9.5
Δp=negligible	2	32	8.4
V=16.7 m/s			
T10	4	57	60.7
Δp=negligible	2	56	49.2
V=68.6 m/s			
B11	4	111	21.8
	3	119	20.4
Δp=49.8 psia	2	114	19.7
V=16.7 m/s	1.5	111	19.2
	1	112	19.0
	.5	112	19.0

TEST CONDITION	PLANE INCHES	MEAN DIA. μM	MEAN VEL. (M/S)
B12	4	120	32.0
	3	126	26.6
Δp=46.8 psia	2	124	23.4
V=33.5 m/s	1.5	135	20.4
	1	125	18.1
	.5	124	17.1
B13	4	101	58.1
	3	100	47.1
Δp=43.9 psia	2	108	37.8
V=68.6 m/s	1.5	108	28.7
	1	106	25.6
	.5	-	16.8
B14	4	102	56.7
	3	104	52.3
Δp=38.0 psia	2	108	42.1
V=79.2 m/s	1.5	112	34.0
	1	107	26.1
	.5	110	16.0
B15	4	116	15.7
	3	116	15.2
Δp=40.0 psia	2	116	14.8
V=22.0 m/s	1.5	114	14.7
	1	115	14.5
	.5	109	14.5
B16	4	117	19.1
	3	117	18.0
Δp=49.8 psia	2	110	17.1
V=16.7 m/s	1.5	106	16.4
	1	108	15.9
	.5	108	15.4
B17	4	107	32.0
	3	111	27.4
Δp=46.8 psia	2	112	25.7
V=33.5 m/s	1.5	119	23.8
	1	114	16.7
	.5	111	14.6
B18	4	105	54.3
	3	106	50.8
Δp=43.9 psia	2	113	36.5
V=68.6 m/s	1.5	114	32.0
	1	118	26.0
	.5	114	16.3

TABLE 5b. - Nozzle Averages

TEST CONDITION	PLANE INCHES	MEAN DIA.μM	MEAN VEL.(M/S)
B19	4	[illegible]	52.4
	3	[illegible]	51.0
Δp=38.0 psia	2	[illegible]	38.4
V=79.2 m/s	1.5	[illegible]	33.8
	1	120	26.8
	.5	120	16.0
B20	4	123	13.5
	3	122	12.6
Δp=40 psia	2	123	12.1
V=22.0 m/s	1.5	128	11.5
	1	119	11.8
	.5	105	11.2
L21	4	111	30.9
	3	111	27.6
Δp=49.8 psia	2	111	23.6
V=16.7 m/s	1.5	111	22.1
	1	126	19.8
	.5	112	18.2
L22	4	109	36.7
	3	102	35.2
Δp=46.8 psia	2	99	30.6
V=33.5 m/s	1.5	100	27.3
	1	108	22.1
	.5	103	17.8
L23	4	106	62.2
	3	104	57.7
Δp=43.9 psia	2	111	48.7
V=68.6 m/s	1.5	117	41.0
	1	108	29.8
	.5	-	18.6
L24	4	106	58.6
	3	107	53.7
Δp=38.0 psia	2	112	42.6
V=79.2 m/s	1.5	109	35.6
	1	110	26.6
	.5	113	16.7
L25	4	116	14.8
	3	116	14.4
Δp=40 psia	2	110	14.1
V=22.0 m/s	1.5	104	13.6
	1	106	13.7
	.5	99	14.3

TEST CONDITION	PLANE INCHES	MEAN DIA.μM	MEAN VEL.(M/S)
S26	4	87	23.3
	3	92	23.7
Δp=89.8 psia	2	92	22.1
V=16.7 m/s	1.5	95	17.8
	1	96	17.2
	.5	90	23.2
S27	4	25	38.8
	3	31	36.0
Δp=86.8 psia	2	25	34.2
V=33.5 m/s	1.5	30	28.0
	1	30	24.2
	.5	28	19.1
S28	4	110	54.4
	3	116	50.9
Δp=83.9 psia	2	101	48.4
V=68.6 m/s	1.5	101	46.4
	1	104	31.5
	.5	97	25.7
S29	4	97	55.0
	3	97	51.1
Δp=78 psia	2	96	47.0
V=79.2 m/s	1.5	100	38.0
	1	120	29.7
	.5	130	22.6
S30	4	41	15.2
	3	40	15.2
Δp=80 psia	2	44	14.8
V=22.0 m/s	1.5	40	14.3
	1	39	13.4
	.5	42	13.7
B031	4	40	19.7
	3	38	18.2
Δp=57.8 psia	2	41	15.7
V=16.7 m/s	1.5	26	14.1
	1	29	13.5
	.5	36	12.1
B032	4	28	37.5
	3	31	32.9
Δp=54.8 psia	2	32	26.6
V=33.5 m/s	1.5	32	22.2
	1	32	18.9
	.5	35	14.1

TABLE 5c. - Nozzle Averages

TEST CONDITION	PLANE INCHES	MEAN DIA.μM	MEAN VEL.(M/S)
B033	4	55	62.8
	3	53	59.9
Δp=51.9 psia	2	53	47.8
V=68.6 m/s	1.5	52	42.5
	1	55	32.1
	.5	51	25.6
B034	4	55	59.2
	3	54	57.9
Δp=46 psia	2	53	47.6
V=79.2 m/s	1.5	55	47.0
	1	52	38.7
	.5	52	29.5
B035	4	31	12.2
	3	33	11.3
Δp=48 psia	2	33	10.1
V=22.0 m/s	1.5	32	9.4
	1	35	8.4
	.5	36	8.7
B036	4	94	21.6
	3	92	20.7
Δp=49.8 psia	2.5	100	19.8
V=16.7 m/s	2	108	20.1
	1.5	105	18.6
	1	99	18.0
B037	4	104	36.4
	3	101	34.3
Δp=46.8 psia	2	102	31.4
V=33.5 m/s	1.5	103	28.4
	1	100	23.6
	.5	83	14.8
B038	4	125	59.7
	3	133	54.8
Δp=43.9 psia	2	120	41.1
V=68.6 m/s	1.5	131	35.8
	1	125	28.8
	.5	129	17.9
B039	4	102	56.2
	3	107	52.1
Δp=38.0 psia	2	122	40.5
V=79.2 m/s	1.5	123	34.8
	1	121	29.9
	.5	-	17.3

TEST CONDITION	PLANE INCHES	MEAN DIA.μM	MEAN VEL.(M/S)
B040	4	123	14.8
	3	115	14.9
Δp=40 psia	2	113	14.4
V=22.0 m/s	1.5	110	14.6
	1	94	13.3
	.5	93	12.3

4.5 Selected Photographs

Individual photographs of several test conditions were taken just prior to droplet data acquisition. Those photographs appear on the following pages (Figure 12). Equipment problems prevented photographs of every test condition from being presented.

B13

B14

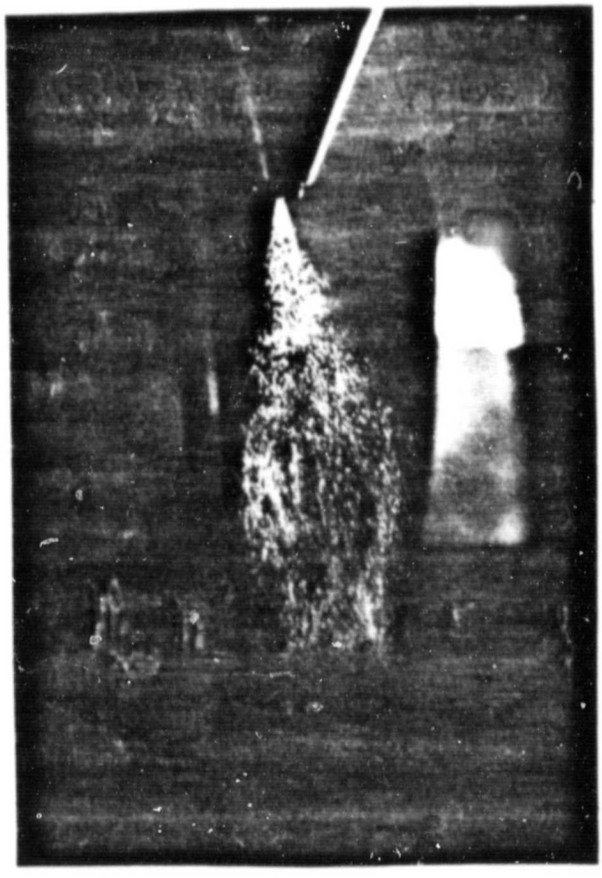

B18

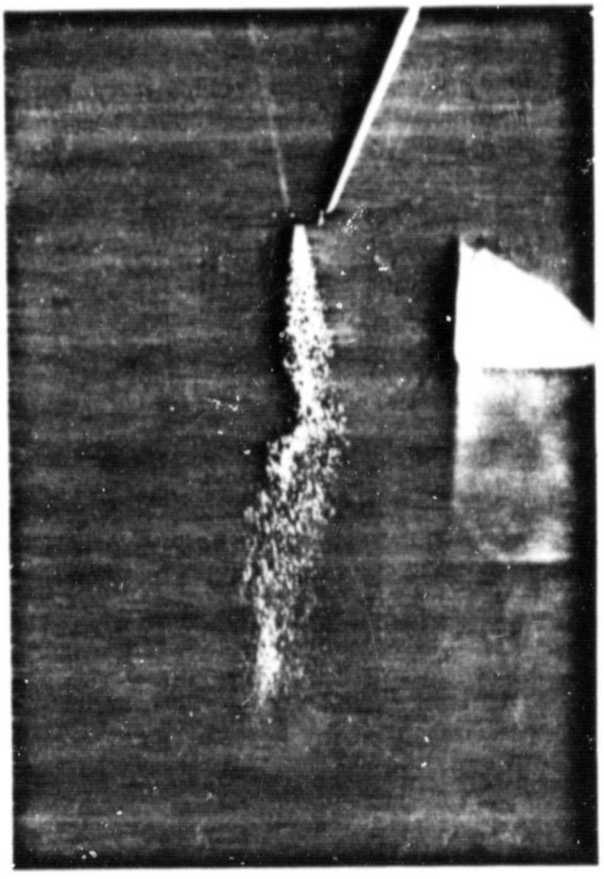

B19

FIGURE 12(a). NOZZLE SPRAY PHOTOGRAPHS

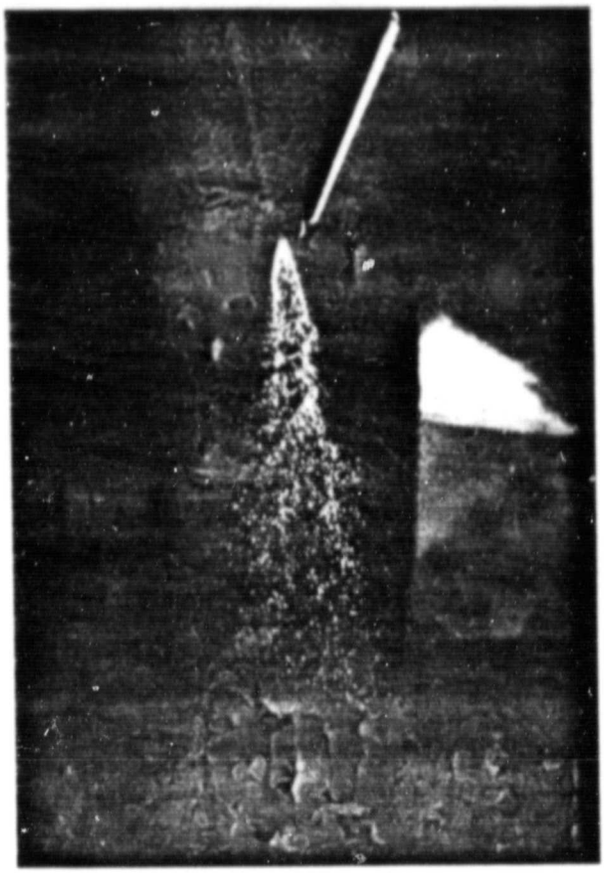

L21
1

L22
1

L23
1

L24

FIGURE 12(b). NOZZLE SPRAY PHOTOGRAPHS

L25

S26

S27

S30

FIGURE 12(c). NOZZLE SPRAY PHOTOGRAPHS

B031

B031

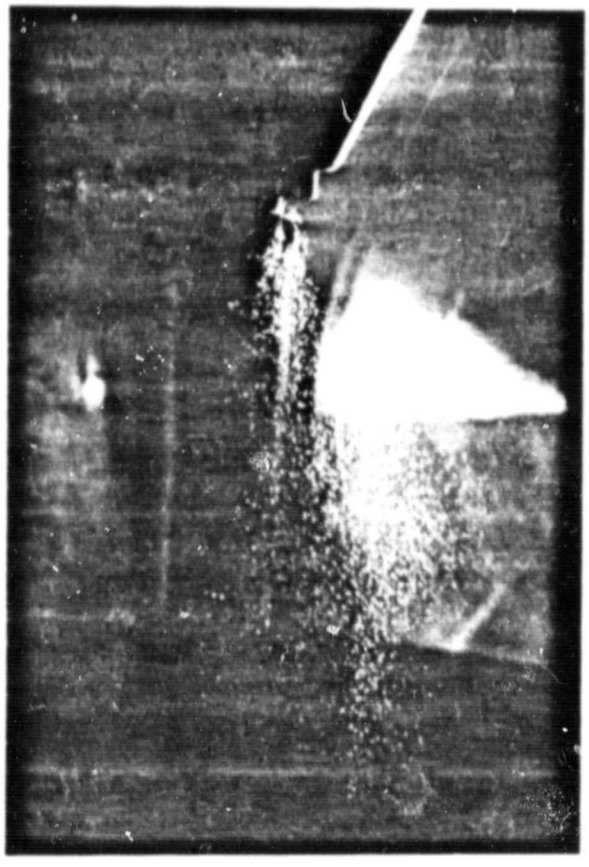

B032

B035

FIGURE 12(d). NOZZLE SPRAY PHOTOGRAPHS

B037

B038

B039

B040

FIGURE 12(e). NOZZLE SPRAY PHOTOGRAPHS

5.0 DISCUSSION

Droplet diameters ranging from 9 to 240 microns were encountered in the 40 nozzle test conditions. Droplet velocities from 8 to over 60 meters/sec. were measured. Nominal air velocities are stated, but actual air velocities were not determined for the modified entrance screen to the test section (see Section 3.3). Air velocity effects on the spray formation are apparent from several photos (e.g., B18, B19, L22, L24, B032, B038). Although the nozzle support tube was designed with the aerodynamics of the flow in mind, the shedding of vortices off the convergent section had drastic effects on the symmetry of the spray. It would have been very difficult to provide a uniform coaxial airflow (at the desired velocities) with objects the size and shape of the injectors located centrally to that flow.

For the purpose of this discussion, the results are categorized by nozzle type: electronic, air-assisted mechanical, and mechanical pintle.

Four (4) electronically operated injectors were investigated (Table 6). All were nearly identical in external design and all were operated in the same manner. A constant voltage (12 VDC) was applied to each to open the injector. All 8 nozzles measured in these tests were operated with continuous flow. Transient effects, due to pulsating fuel flow, on droplet size were not studied. The droplet size data obtained for the four electronic injectors showed remarkable consistency. No trends in size were observed with distance from the injector exit.

TEST POINT	NOZZLE	ΔP(NOZZLE) (psi)	NOMINAL AIR VELOCITY (m/s)	PLANAR DATA											
				DROPLET SIZE (MICRONS)						DROPLET VELOCITY (m/s)					
				0.5	1.0	1.5	2.0	3.0	4.0	0.5	1.0	1.5	2.0	3.0	4.0
B11	BENDIX 1606771	49.8	16.7	112	112	111	114	119	111	19.0	19.0	19.2	19.7	20.4	21.8
B12		46.8	33.5	124	125	135	124	126	120	17.1	18.1	20.4	23.4	26.6	32.0
B13		43.9	68.6	-	106	108	108	100	101	16.8	25.6	28.7	37.8	47.1	58.1
B14		38.0	79.2	110	107	112	108	104	102	16.0	26.1	34.0	42.1	52.3	56.7
B15		40.0	22.0	109	115	114	116	116	116	14.5	14.5	14.7	14.8	15.2	15.7
B16	BENDIX 1607247	49.8	16.7	108	108	106	110	117	117	15.4	15.9	16.4	17.1	18.0	19.1
B17		46.8	33.5	111	114	119	112	111	107	14.6	16.7	23.8	25.7	27.4	32.0
B18		43.9	68.6	114	118	114	113	106	105	16.3	26.0	32.0	36.5	50.8	54.3
B19		38.0	79.2	120	120	122	121	112	105	16.0	26.8	33.8	38.4	51.0	52.4
B20		40.0	22.0	105	119	128	123	122	128	11.2	11.8	11.5	12.1	12.6	13.5
L21	LUCAS 073143	49.8	16.7	112	126	111	111	111	111	18.2	19.8	22.1	23.6	27.6	30.9
L22		46.8	33.5	103	108	100	99	102	109	17.8	22.1	27.3	30.6	35.2	36.7
L23		43.9	68.6	-	108	117	111	104	106	18.6	29.8	41.0	48.7	57.7	62.2
L24		38.0	79.2	113	110	109	112	107	106	16.7	26.6	35.6	42.6	53.7	58.6
L25		40.0	22.0	99	106	104	110	116	116	14.3	13.7	13.6	14.1	14.4	14.8
B036	BOSCH 0280-150-151	49.8	16.7	99	105	108	100	92	94	18.0	18.6	20.1	19.8	20.7	21.6
B037		46.8	33.5	83	100	103	102	101	104	14.8	23.6	28.4	31.4	34.3	36.4
B038		43.9	68.6	129	125	131	120	133	125	17.9	28.8	35.8	41.1	54.8	59.7
B039		38.0	79.2	-	121	123	122	107	102	17.3	29.9	34.8	40.5	52.1	56.2
B040		40.0	22.0	93	94	110	113	115	123	12.3	13.3	14.6	14.4	14.9	14.8

ΔP(NOZZLE) = P(FUEL) - P(TEST SECTION)

TABLE 6. ELECTRONIC NOZZLES

Velocity data, however, generally increased with downstream distance. Velocities at the 0.5" plane (very near injector exit) showed an increase with increasing nozzle pressure drop.

Two (2) air-assisted mechanical injectors were investigated (Table 7). These nozzles required the addition of atomizing shroud air mixed with the fuel in the injector body. These nozzles produced significantly smaller sized droplets than the electronic nozzles. An increase in shroud air pressure produced smaller droplets (e.g. T9). Again, each nozzle produced nearly consistent droplet sizes at all downstream planes and for most operating conditions. The smaller droplets of these nozzles responded more quickly to the air velocities.

Data missing from Table 7 was not obtained due to a lack of time to complete the experiment. Test point B4 did not produce a spray. The fuel exited the injector as a jet without atomizing. Unfortunately, photographs for the test conditions were unavailable.

Two (2) mechanical pintle injectors were investigated (Table 8). These injectors produced relatively different droplet sizes under different test conditions. The nozzle pressure drop did not change significantly between conditions. From the available photographs, the spray sheet of test point S27 (Figure 12c) appears to be undergoing breakup in about one-half the distance as the spray sheet of test point S26 (Figure 12c). This effect may corrrelate with the difference in droplet size. Droplet velocities are consistent with the nominal air velocities.

Experimental error cannot be rejected as a possibility in explaining the size differences. Data on test points S27, S30, B031, B032, and

TEST POINT	NOZZLE	ΔP(NOZZLE) (psi)	ΔP(SHROUD) (psi)	NOMINAL AIR VELOCITY (m/s)	PLANAR DATA (DROPLET SIZE (MICRONS)						DROPLET VELOCITY (m/s)					
					0.5	1.0	1.5	2.0	3.0	4.0	0.5	1.0	1.5	2.0	3.0	4.0
B1	BENDIX 74151	9.0	9.0	16.7	-	45	45	43	40	34	-	32.0	31.0	27.0	24.0	22.0
B2		7.2	2.7	68.6	50	52	55	55	55	55	18.0	33.0	40.0	45.8	57.1	60.8
B3		7.9	0.9	79.2	53	55	56	58	58	60	17.4	34.0	41.4	46.3	53.0	56.2
B4		0.0+	0.0	16.7	-	-	-	-	-	-	-	-	-	-	-	-
B5		0.0+	0.0	68.6	-	36	40	41	41	41	26.0	27.3	42.3	47.2	56.0	58.7
T6	TCM 63308-13E	5.6	5.2	16.7	-	-	-	40	-	43	-	-	-	13.3	-	15.1
T7		1.8	0.4	68.6	-	-	-	55	-	57	-	-	-	46.0	-	58.6
T8		5.0	1.1	79.2	-	-	-	44	-	44	-	-	-	39.4	-	51.5
T9		0.0+	8.4	16.7	-	-	-	29	-	32	-	-	-	8.4	-	9.5
T10		0.0+	0.3	68.6	-	-	-	56	-	57	-	-	-	49.2	-	60.7

ΔP(NOZZLE) = P(FUEL) - P(TEST SECTION)

ΔP(SHROUD) = Pair(SHROUD) - P(TEST SECTION)

TABLE 7. AIR-ASSISTED MECHANICAL NOZZLES

TEST POINT	NOZZLE	Δ P (NOZZLE) (psi)	NOMINAL AIR VELOCITY (m/s)	PLANAR DATA											
				DROPLET SIZE (MICRONS)						DROPLET VELOCITY (m/s)					
				0.5	1.0	1.5	2.0	3.0	4.0	0.5	1.0	1.5	2.0	3.0	4.0
S26	Simmonds 571341	89.8	16.7	90	96	95	92	92	87	23.2	17.2	17.8	22.1	23.7	23.3
S27		86.8	33.5	28	30	30	25	31	25	19.1	24.2	28.0	34.2	36.0	38.8
S28		83.9	68.6	97	104	101	101	116	110	25.7	31.5	46.4	48.4	50.9	54.4
S29		78.0	79.2	130	120	100	96	97	97	22.6	29.7	38.0	47.0	51.1	55.0
S30		80.0	22.0	42	39	40	44	40	41	13.7	13.4	14.3	14.8	15.2	15.2
B031	Bosch 0437-502-004	57.8	16.7	36	29	26	41	38	40	12.1	13.5	14.1	15.7	18.2	19.7
B032		54.8	33.5	35	32	32	32	31	28	14.1	18.9	22.2	26.6	32.9	37.5
B033		51.9	68.6	51	55	52	53	53	55	25.6	32.1	42.5	47.8	59.9	62.8
B034		46.0	79.2	52	52	55	53	54	55	29.5	38.7	47.0	47.6	57.9	59.2
B035		48.0	22.0	36	35	32	33	33	31	8.7	8.4	9.4	10.1	11.3	12.2

Δ P(NOZZLE) = P(FUEL) - P(TEST SECTION)

TABLE 8. MECHANICAL PINTLE NOZZLES

B035 were obtained in the initial stages of the test. There is reason to believe that the Spectron visibility processor's prototype auto gain control was not operating properly. The system was set by the auto gain circuitry to be more sensitive to smaller droplets to the apparent exclusion of larger droplets present in the spray. This problem was corrected, but the effect on data collected up to that time was not determined.

No error analysis of the data was provided because of time limitations. Planned publication of synoptic results will include such analysis.

6.0 CONCLUSIONS

Measurements were completed on the droplet size and velocities of commercial fuel injectors. These data were obtained under representative operating conditions. The spatial droplet size, velocity and the size-velocity correlations produced under this program represents a unique characterization of spray nozzles that was, heretofore, unavailable.

Although there are some discrepancies in the results, described in the discussion, the voluminous amount of data presented is in most part believed to be accurate. Primarily, the early results were the only data in question. The consistency in droplet size for the various types of nozzles (electronic, air-assist mechanical, and the mechanical pintle) was reassuring.

Some airflow instability affects were apparent in these measurements. However, the airflow velocity did not produce significant changes in the droplet size distribution, only in their velocity. In future measurements, it would be useful to better model the manifold or other nozzle environment.

The Droplet Sizing Interferometer experienced little difficulty in producing the spray size and velocity measurements. Under some conditions of inefficient atomization, the size distributions at the 0.5 inch station were suspect. This was in part due to incomplete breakup of the fuel ligaments and in part due to excessively high number densities. Future measurements of both the air and the fuel velocities would be useful to evaluate air-fuel mixing. Also, more complex fluid dynamics

consisting of swirling flows should be studied. In these applications, frequency shifting should be used to resolve reversed flows and to more accurately determine the radial velocity component. Overall, the measurement technique was proved to be capable of providing complete spray characterization data.

APPENDIX I

TEST POINT CONDITIONS

TEST POINT CONDITIONS

TEST POINT	EXPECTED TEST MATRIX VALUES					ACTUAL INLET AIR									ACTUAL SHROUD AIR		ACTUAL FUEL		
									NORTH			SOUTH							
	FUEL FLOW (lbm/hr)	FUEL PRESS (psig)	TUNNEL PRESS ("Hg)	AIR SPEED (f/s)	SHROUD PRESS ("Hg)	$\Delta P_{orifice}$ ("H_2O)	$P_{upstream\ orifice}$ (psi)	$\dot{M}_{air}$ (lbm/sec)	P_{total} ("Hg)	P_{static} ("Hg)	T (°F)	P_{total} ("Hg)	P_{static} ("Hg)	T (°F)	P_{air} ("Hg)	T (°F)	P_{nozzle} (psig)	$\dot{M}_{fuel}$ [cps/(lbm/hr)]	T (°F)
B1	1.2	*	(-18.4)	55	0.0	3.7	80	.5	-18.2	-18.4	54	-18.2	-18.4	54	0.0	–	*	*/1.2	70
B2	11.6	4.5	(-5.4)	225	0.0	60.0	80	4.6	-5.2	-5.4	52	-5.2	-5.4	52	0.0	–	*	220/11.6	75
B3	20.0	7.0	(-1.9)	260	0.0	75.0	80	5.2	-1.7	-1.9	50	-1.7	-1.9	50	0.0	–	14	400/20	75
B4	1.2	*	0.0	55	0.0	- - - -	- - - -	- - - -	- - - -	- - - Spray did not atomize - - -					- - - -	- - - -	- - - -	- - - -	- -
B5	11.6	4.5	0.0	225	0.0	85.0	80	5.5	.15	0.0	40	.15	0.0	40	0.0	–	6	210/11.5	70
T6	1.3	*	(-11.4)	55	-0.9	.7	80	.5	-11.3	-11.4	51	-11.3	-11.4	51	-0.9	60	*	*/1.3	65
T7	13.0	2.5	(2.7)	225	3.5	100.0	80	6.0	2.9	2.7	48	2.9	2.7	48	3.5	60	10	250/13	65
T8	24.0	8.2	(6.6)	260	8.9	100.0	80	6.0	6.1	6.0	46	6.1	6.0	46	8.9	60	29	500/24.0	60
T9	1.3	*	0.0	55	17.0	.7	80	.5	.1	0.0	60	.1	0.0	60	17.0	60	*	*/1.3	65
T10	13.0	2.5	0.0	225	0.7	87.0	80	5.7	.1	0.0	51	.1	0.0	51	1.0	60	10	250/13	65
B11	39.7	40.0	(-19.9)	55	–	3.7	80	.5	-19.7	-19.9	59	-19.7	-19.9	59	–	–	40	720/34	70
B12	39.7	40.0	(-13.9)	110	–	60.0	80	2.0	-13.7	-13.9	63	-13.7	-13.9	63	–	–	40	680/32	70
B13	39.7	40.0	(-7.9)	225	–	42.0	90	4.1	-7.7	-7.9	64	-7.7	-7.9	64	–	–	40	675/32	75
B14	39.7	40.0	(+4.1)	260	–	100.0	80	6.0	4.2	4.1	66	4.2	4.1	66	–	–	40	630/30	75
B15	39.7	40.0	0.0	†Intermediate	–	15.0	80	1.0	.15	.1	59	.15	.1	59	–	–	40	630/30	70
B16	49.9	40.0	(-19.9)	55	–	3.7	80	.5	-19.7	-19.9	64	-19.7	-19.9	64	–	–	40	825/39	75
B17	49.9	40.0	(-13.9)	110	–	60.0	80	2.0	-13.7	-13.9	54	-13.7	-13.9	54	–	–	40	800/38	75

NOTE: All pressures are gauge

* Fuel flow too low to register these values, flow set via Rotometer

† Test Point set via air mass flowrate. Approximate velocity 75 f/s.

TEST POINT CONDITIONS

TEST POINT	EXPECTED TEST MATRIX VALUES					ACTUAL INLET AIR									ACTUAL SHROUD AIR		ACTUAL FUEL		
									NORTH			SOUTH							
	FUEL FLOW (lbm/hr)	FUEL PRESS (psig)	TUNNEL PRESS ("Hg)	AIR SPEED (f/s)	SHROUD PRESS ("Hg)	$\Delta P_{orifice}$ ("H_2O)	$P_{upstream\ orifice}$ (psi)	$\dot{M}_{air}$ (lbm/sec)	P_{total} ("Hg)	P_{static} ("Hg)	T (°F)	P_{total} ("Hg)	P_{static} ("Hg)	T (°F)	P_{air} ("Hg)	T (°F)	P_{nozzle} (psig)	$\dot{M}_{fuel}$ [cps/(lbm/hr)]	T (°F)
B18	49.9	40.0	(-7.9)	225	-	43.0	90	4.1	-7.7	-7.9	53	-7.7	-7.9	53	-	-	40	730/34.5	70
B19	49.9	40.0	(4.1)	260	-	100.0	80	6.0	4.2	4.1	55	4.2	4.1	55	-	-	40	680/32	75
B20	49.9	40.0	0.0	†Inter-mediate	-	17.0	70	1.0	.15	.10	60	.15	.10	60	-	-	40	730/34	75
L21	41.8	40.0	(-19.9)	55	-	15.0	80	1.0	-19.7	-19.9	83	-19.7	-19.9	83	-	-	40	710/33.5	75
L22	41.8	40.0	(-13.9)	110	-	60.0	80	2.0	-13.7	-13.9	55	-13.7	-13.9	55	-	-	40	670/32	75
L23	41.8	40.0	(-7.9)	225	-	42.0	90	4.1	-7.7	-7.9	48	-7.7	-7.9	48	-	-	40	650/31	75
L24	41.8	40.0	(+4.1)	260	-	100.0	80	6.0	4.2	4.1	50	4.2	4.1	50	-	-	40	580/28	75
L25	41.8	40.0	0.0	†Inter-mediate	-	15.0	80	1.0	.3	.2	64	.3	.2	64	-	-	40	630/30	75
S26	221.0	80.0	(-19.9)	55	-	3.7	80	.5	-19.7	-19.9	62	-19.7	-19.9	62	-	-	80	1050/48.5	80
S27	221.0	80.0	(-13.9)	110	-	60.0	80	2.0	-13.7	-13.9	65	-13.7	-13.9	65	-	-	80	880/42	80
S28	221.0	80.0	(-7.9)	225	-	42.0	90	4.1	-7.7	-7.9	50	-7.7	-7.9	50	-	-	80	920/43	80
S29	221.0	80.0	(4.1)	260	-	100.0	80	6.0	4.2	4.1	45	4.2	4.1	45	-	-	80	900/42	70
S30	221.0	80.0	0.0	†Inter-mediate	-	15.0	80	1.0	0.0	0.0	61	0.0	0.0	61	-	-	80	790/37	80
B031	10.0	48.0	(-19.9)	55	-	3.5	80	.5	-19.8	-19.9	68	-19.8	-19.9	68	-	-	48	**	75
B032	10.0	48.0	(-13.9)	110	-	60.0	80	2.0	-13.7	-13.9	54	-13.7	-13.9	54	-	-	48	**	75
B033	10.0	48.0	(-7.9)	225	-	45.0	90	4.2	-7.7	-7.9	61	-7.7	-7.9	61	-	-	48	125/8	75
B034	10.0	48.0	(4.1)	260	-	100.0	80	6.0	4.3	4.1	75	4.3	4.1	75	-	-	48	**	75

NOTE: All pressures are gauge

† Test Point set via air mass flowrate. Approximate velocity 75 f/s.

@ Fuel flow too low to register these values, flow set via Rotometer
** Equipment Failure

TEST POINT CONDITIONS

TEST POINT	EXPECTED TEST MATRIX VALUES					ACTUAL INLET AIR									ACTUAL SHROUD AIR		ACTUAL FUEL		
									NORTH			SOUTH							
	FUEL FLOW (lbm/hr)	FUEL PRESS (psig)	TUNNEL PRESS ("Hg)	AIR SPEED (f/s)	SHROUD PRESS ("Hg)	$\Delta P_{orifice}$ ("H_2O)	$P_{upstream\ orifice}$ (psi)	$\dot{M}_{air}$ (lbm/sec)	P_{total} ("Hg)	P_{static} ("Hg)	T (°F)	P_{total} ("Hg)	P_{static} ("Hg)	T (°F)	P_{air} ("Hg)	T (°F)	P_{nozzle} (psig)	$\dot{M}_{fuel}$ [cps/(lbm/hr)]	T (°F)
B035	10.0	48	0.0	†Intermediate	–	15.0	80	1.0	0.0	0.0	50	0.0	0.0	50	–	–	48	**	74
B036	25.1	40	(-19.9)	55	–	5.3	80	.5	-19.7	-19.9	80	-19.7	-19.9	80	–	–	40	229/73	80
B037	25.1	40	(-13.9)	110	–	11.5	80	2.0	-13.7	-13.9	58	-13.7	-13.9	58	–	–	40	430/21	75
B038	25.1	40	(-7.9)	225	–	45.0	90	4.2	-7.6	-7.9	59	-7.6	-7.9	59	–	–	40	430/21	75
B039	25.1	40	(4.1)	250	–	100.0	80	6.0	+4.3	4.1	49	4.3	4.1	49	–	–	40	380/19	75
B040	25.1	40	0.0	†Intermediate	–	2.75	80	1.0	+.05	0.0	50	+.05	0.0	50	–	–	40	400/40	75

NOTE: All pressures are gauge

* Fuel flow too low to register these values, flow set via Rotometer
** Equipment Failure

† Test Point set via air mass flowrate.
Approximate velocity 75 f/s.